pharmaceuticals

MDPI

Article

An Integrated NONMEM-Based Framework for Ticagrelor Exposure–PRU Modeling and Patient-Level Outcome Prediction Assessment

Songrui Du [1,2], Jingcheng Chen [1,2], Dongyang Liu [1,2,3,4,*] and Cheng Cui [1,2,*]

[1] Drug Clinical Trial Center, Department of Pharmacy, Peking University Third Hospital, Beijing 100191, China; dusongrui@bjmu.edu.cn (S.D.)
[2] Center of Clinical Medical Research, Institute of Medical Innovation and Research, Peking University Third Hospital, Beijing 100191, China
[3] State Key Laboratory of Vascular Homeostasis and Remodeling, NHC Key Laboratory of Cardiovascular Molecular Biology and Regulatory Peptides, Peking University, Beijing 100191, China
[4] Beijing Key Laboratory of Cardiovascular Receptors Research, Peking University Third Hospital, Beijing 100191, China
* Correspondence: liudongyang@bjmu.edu.cn (D.L.); cuicheng1226@163.com (C.C.)

Abstract

Background/Objectives: Ticagrelor reduces ischemic events in acute coronary syndrome (ACS) but may increase bleeding in susceptible patients. We used a population PK and PK/PD model to describe ticagrelor exposure and platelet reactivity unit (PRU) dynamics and assessed whether model-predicted PRU improved prediction of subsequent outcomes in a patient-level analysis. **Methods**: We collated published evidence from 39 ticagrelor clinical studies (172 group-level datasets). The final population PK and indirect-response PK/PD models for ticagrelor, AR-C124910XX, and PRU were implemented in NONMEM with a two-compartment structure, three transit absorption compartments, and prespecified covariate relationships. Model-predicted PRU from recorded prescription exposure was linked to subsequent outcomes in a de-identified UK Biobank cohort using a prespecified 90-day landmark analysis. Cox models with clinical variables, recorded medication exposure, and model-predicted PRU were compared; a 30-day landmark analysis was used for sensitivity analysis. **Results**: The final model retained a two-compartment structure with three transit absorption compartments and quantified age, disease status, concomitant aspirin, and fasting effects on exposure. The indirect-response model linked combined parent-metabolite molar concentration to continuous PRU dynamics. In 731 UK Biobank participants, the 90-day ischemic, bleeding, and all-cause death analyses included 112, 48, and 129 events, respectively. Adding model-predicted PRU did not show stable incremental discrimination; all paired-bootstrap intervals for C-index and Brier-score increments crossed zero. **Conclusions**: We established a NONMEM-based framework linking ticagrelor dosing, exposure, and PRU dynamics to patient-level outcome prediction assessment. Although incremental predictive benefit was not established in the current cohort, the framework provides a basis for further evaluation using paired measured PK, PRU, and clinical outcome data before clinical application.

Keywords: ticagrelor; model-based meta-analysis; platelet reactivity units; population pharmacokinetics; pharmacokinetic-pharmacodynamic modeling; clinical outcome prediction

Check for updates

Academic Editors: Arquimedes Gasparotto Junior and Donato Colangelo

Received: 14 September 2026
Revised: 10 October 2026
Accepted: 4 November 2026
Published: 9 November 2026

Copyright: © 2026 by the authors. Licensee MDPI, Basel, Switzerland. This article is an open access article distributed under the terms and conditions of the Creative Commons Attribution (CC BY) license.

1. Introduction

Patients with acute coronary syndrome (ACS) and those undergoing percutaneous coronary intervention (PCI) remain at substantial risk of recurrent ischemic events and death long after the index event. Dual antiplatelet therapy (DAPT) is the cornerstone of secondary prevention, with P2Y12 receptor antagonists playing a pivotal role in balancing therapeutic benefits and risks [1–4]. Ticagrelor, a potent reversible P2Y12 antagonist, has demonstrated superior protection against major adverse cardiovascular events (MACE) in landmark trials (PLATO, PEGASUS-TIMI 54) [1,5–7]. However, these ischemic benefits are counterbalanced by a significant increase in major bleeding, an imbalance that is particularly pronounced in older adults (>65 years), East Asian populations, and individuals with high bleeding risk (e.g., high PRECISE-DAPT scores) [8–10]. Despite strong guideline recommendations for ticagrelor in ACS/PCI patients, the lack of population-specific dosing evidence and a ticagrelor-tailored platelet reactivity threshold significantly hinders its real-world utility in these high-bleeding-risk subgroups [11].

Platelet reactivity units (PRUs), measured by the VerifyNow assay (Accumetrics, San Diego, CA, USA), are pharmacodynamic markers of P2Y12 inhibition and have been associated with ischemic and bleeding outcomes in observational and interventional studies [12–14]. However, the clinical meaning of a model-predicted PRU depends on the underlying treatment record, patient population, endpoint definition, and calibration of the outcome model. Existing platelet reactivity thresholds are not established treatment targets for ticagrelor and should not be used to infer individualized dose changes without prospective evidence [15–17].

Previous studies of ticagrelor's pharmacokinetics (PK) and pharmacodynamics (PD) have identified covariates that affect drug exposure and platelet inhibition. Few studies have examined whether a model-predicted PRU trajectory improves prediction of subsequent patient-level outcomes. Studies in Chinese healthy volunteers and patients with stable coronary disease also show that population and clinical context must be considered [18,19], particularly when bleeding susceptibility differs by age or ethnicity.

We therefore conducted a model-based meta-analysis of ticagrelor PK and PD data and a prespecified patient-level outcome prediction assessment in the UK Biobank. We aimed to (1) develop a NONMEM population PK and sequential PK/PD model linking ticagrelor dosing to continuous PRU trajectories, (2) test whether model-predicted PRU adds predictive information beyond clinical and recorded medication variables, and (3) identify the requirements for future external validation. We did not seek to establish a ticagrelor-specific PRU threshold or treatment interval.

2. Results

2.1. Data Overview

The collated model-development dataset comprised 39 published clinical studies (172 group-level datasets) from 2010 to 2023, with a total sample size of 2749 participants. These studies cover healthy volunteers, ACS/PCI patients, single-/multiple-dose regimens, and both East Asian and non-East Asian populations with diverse bleeding risk profiles.

2.2. PopPK Model and Key Covariates

The final NONMEM model used a dosing compartment followed by three transit absorption compartments for oral ticagrelor, two-compartment distribution for the parent drug, parent-clearance-linked formation of AR-C124910XX, and two-compartment distribution for the metabolite (Figure 1). Variability in the model-development records was represented with exponential random effects and was not interpreted as patient-specific IIV; residual error was modeled on a log-additive scale.

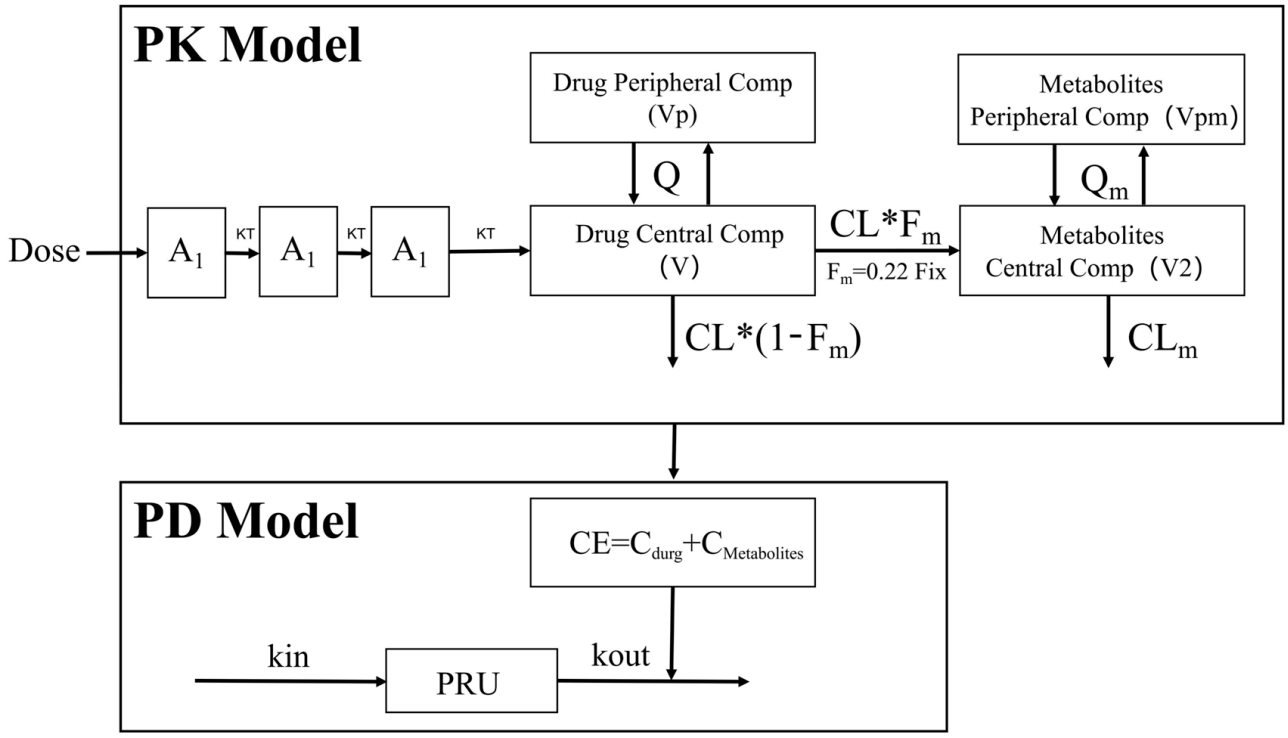


Figure 1. Structural population pharmacokinetic/pharmacodynamic (PK/PD) model for ticagrelor and its active metabolite AR-C124910XX. The implemented absorption chain is Aa/DEPOT → T1 → T2 → T3 → parent-drug central compartment, with KT governing each transfer. The PK component includes a two-compartment parent-drug model, clearance-linked metabolite formation with a fixed typical Fm of 0.22 and a retained age-group effect, and a two-compartment metabolite model. The PD component is an indirect-response model in which combined parent and metabolite molar concentrations increase the platelet reactivity unit (PRU) loss term, Kout × PRU × (1 + EFF), thereby lowering the PRU state; they do not directly inhibit Kin.

Point estimates and structural relationships were aligned to the final fixed-parameter NONMEM control stream. Relative standard errors (RSEss, expressed as percentages) summarize the precision of parameter estimates and are distinct from the variability represented by random effects. RSE and shrinkage summaries are retained from the model-development estimation table where available; confidence intervals are marked unavailable when the retained output did not provide both limits. The dimensionless reference-group typical Fm was fixed at 0.2200; its age-group effect was reported separately. In the model-development control streams, Fm also includes an exponential random effect; the patient-level typical prediction sets random effects to zero while retaining the age-group relationship.

The final PK/PD model included effects of age (>65 years), disease status (ACS/PCI), concomitant aspirin use, and fasting status. Relative to the reference categories, age > 65 years was associated with 8.7% lower clearance (CL) and 5.9% lower metabolite formation fraction (Fm); concomitant aspirin was associated with 35.7% lower CL; non-fasting was associated with 45.0% higher central volume (V) and 56.0% lower intercompartmental clearance (Q); and ACS/PCI status was associated with 11.9% lower CL, 19.0% higher peripheral volume (Vp), and 84.8% higher EC_{50} (Table 1). These relationships were used in the simulation scenarios and the patient-level prediction model.

Table 1. Final PK/PD parameter estimates and uncertainty summaries.

Parameter	Unit	Estimate	RSE (%)	Shrinkage (%)	Interval Availability *	Explanation
V	L	139.6325	5.6847	10.2920	Not available	Ticagrelor central compartment volume
CL	L/h	23.2788	3.7967	8.9047	Not available	Clearance
K_T	/h	3.8602	5.8532	21.7938	Not available	First-order transfer rate constant along the absorption transit chain
V_p	L	83.9282	12.1145	21.7089	Not available	Ticagrelor peripheral compartment volume
Q	L/h	9.3333	17.1236	37.7420	Not available	Represents the intercompartmental clearance between the central and peripheral compartments of ticagrelor
dCLPTTYPE1	-	−0.1263	315.3879	-	Not available	The impact of disease on clearance rate
dCLASP1	-	−0.4417	85.9897	-	Not available	Model-estimated association of concomitant aspirin with CL
dV_pPTTYPE1	-	0.1743	193.6075	-	Not available	The impact of disease on Vp
dVFAFE1	-	0.3717	22.6037	-	Not available	Model-estimated effect of non-fasting status on V
dQFAFE1	-	−0.8207	45.0277	-	Not available	Model-estimated effect of non-fasting status on Q
dCLAGEE1	-	−0.0910	127.3042	-	Not available	The impact of age on clearance rate
Residual Error 1	-	0.1837	2.1849	-	Not available	Log-scale residual SD for ticagrelor
V_{pm}	L	27.9742	28.9038	41.3023	Not available	Metabolite peripheral compartment volume
V_2	L	2.7403	34.1228	50.5458	Not available	Metabolite central compartment volume
CL_m	L/h	10.8328	6.3322	54.4352	Not available	Metabolite clearance
Q_m	L/h	4.2089	12.1491	48.9928	Not available	Clearance between metabolite compartments
F_m	-	0.2200 (fixed)	Not estimated	Not estimated	Not applicable	Fixed reference-group typical metabolite formation fraction
dF_mAGEE1	-	−0.0610	3.2672	-	Not available	Model-estimated age-group effect on Fm
Residual Error 2	-	0.1530	28.9038	-	Not available	Log-scale residual SD for metabolite
EC_{50}	nmol/L	214.9238	117.4771	31.0150	Not available	Half-maximal effective concentration
E_{max}	-	2.2855	34.9698	30.2857	Not available	Maximum fractional increase in the PRU loss-rate constant
K_{out}	/h	1.1566	100.3929	96.9002	Not available	PRU loss rate
K_{in}	PRU/h	313.1724	102.2894	89.9550	Not available	PRU production rate
dEC_{50}AGEE1	-	0 (fixed)	Not estimated	Not estimated	Not applicable	Age effect on EC_{50} was fixed to zero
dEC_{50}PTTYPE1	-	0.6139	124.9929	-	Not available	The impact of disease on EC_{50}
Residual Error 3	-	0.13629	29.1561	-	Not available	Log-scale residual SD for PRU

Note. RSE (%) describes parameter estimation precision, not interindividual variability. Intervals were unavailable in the retained output; fixed parameters have no estimated RSE or interval. Residual errors 1–3 are dimensionless standard deviations (SDs) in $Y = Ypred \times \exp(\varepsilon)$, where ε is normally distributed with mean 0 and variance SD^2. They are not variances or RSE values. The asterisk indicates that intervals were unavailable in the retained model output.

2.3. PK/PD Relationship and PRU Dynamics

The indirect-response PK/PD model used the total molar concentrations of ticagrelor and AR-C124910XX to describe PRU dynamics. The estimated half-maximal effective concentration (EC_{50}) was 214.9 nmol/L, and E_{max} was 2.29, representing the maximum fractional increase in the PRU loss-rate constant. PRU production rate (Kin) was 313.2 PRU/h, and the baseline loss-rate constant (Kout) was 1.16/h (Table 1).

Ticagrelor exposure was inversely associated with PRU. Steady-state PRU decreased gradually with increasing total molar concentration, reflecting the drug's gradual onset and offset of platelet inhibition. ACS patients exhibited reduced PD sensitivity (EC_{50} increased by 84.8%) compared with healthy volunteers. Age-related exposure differences were associated with deeper platelet inhibition at the same nominal dose.

2.4. Model Implementation and Diagnostic Provenance

The final parameter state was used in the patient-level NONMEM prediction run. GOF and VPC diagnostics for concentration and PRU data (Figures 2 and 3) came from model development and were not regenerated in that run. No numerical threshold from these figures was used in the outcome analysis. The patient-level run used fixed parameters and did not repeat parameter estimation, structural model comparison, or model qualification.

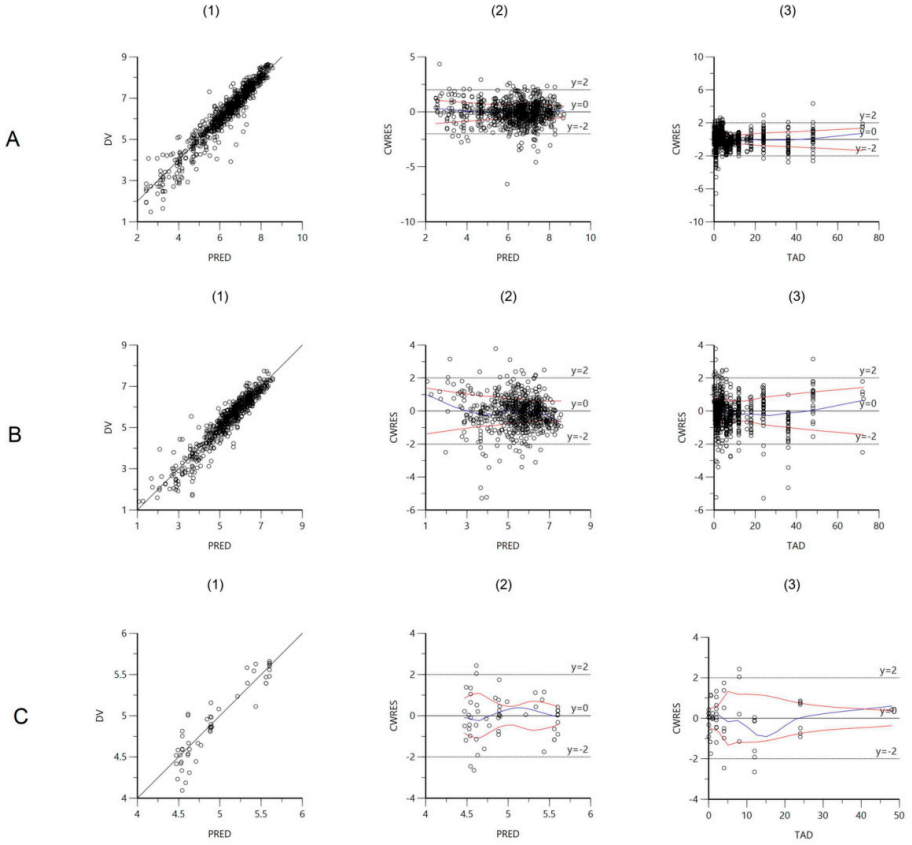


Figure 2. Panels (**A**–**C**) show parent-drug PK, metabolite PK, and PRU PD, respectively; within each row, panels (**1**–**3**) show DV versus PRED, CWRES versus PRED, and CWRES versus TAD. Black symbols denote observations; diagonal and horizontal reference lines indicate identity, zero, and ±2 residuals. Blue curves show smoothed residual trends, and red curves show their confidence bounds. Goodness-of-fit plots for parent-drug PK, metabolite PK, and PRU PD from the final model-development analysis. Patient-level PRU predictions used the fixed-parameter NONMEM implementation; these diagnostics were not regenerated in the patient-level run.

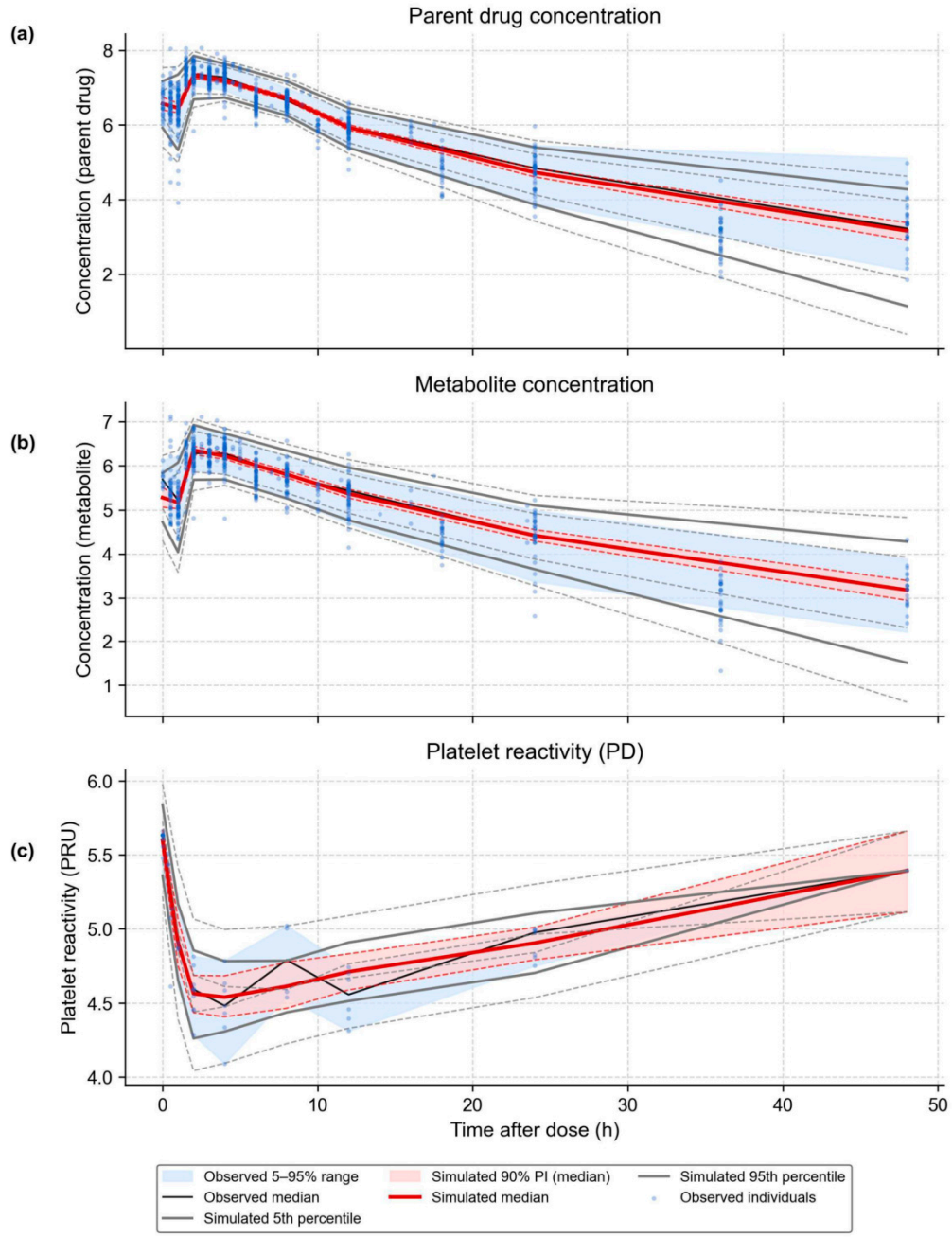


Figure 3. Gray solid lines show the simulated 5th and 95th percentiles; gray dotted lines indicate their simulation-based 95% confidence limits. Red shading and dashed lines show the simulated 90% prediction interval; the red solid line shows its median. Visual predictive checks for (**a**) parent-drug ticagrelor plasma concentrations, (**b**) plasma concentrations of AR-C124910XX, and (**c**) platelet reactivity expressed as PRU from the final model-development analysis. Patient-level PRU predictions used the fixed-parameter NONMEM implementation and did not regenerate these checks. Blue shading shows the observed 5th–95th percentile range; blue symbols and lines show observed individuals and medians; red and black elements show the corresponding simulated summaries.

2.5. Model-Based PRU Simulation Results

Simulations across 16 predefined clinical profiles described dose- and profile-dependent distributions of model-predicted PRU for ticagrelor maintenance regimens of 90, 60, and 45 mg twice daily (Table 2 and Figure 4). These outputs describe model behavior and do not represent observed outcomes or clinical dose recommendations.

Table 2. Predefined model-based simulation scenarios.

Scenario ID	Age Group	Disease Status	Fasting Status	Concomitant Aspirin	Clinical Profile Summary
1	≤65 years	Reference (0)	Fasting	No	Fasting only
2	≤65 years	Reference (0)	Non-fasting	No	Reference covariate combination
3	>65 years	Reference (0)	Fasting	No	Older age + fasting
4	≤65 years	Patient (1)	Fasting	No	Patient status + fasting
5	≤65 years	Reference (0)	Fasting	Yes	Fasting + aspirin
6	>65 years	Reference (0)	Non-fasting	No	Older age only
7	≤65 years	Patient (1)	Non-fasting	No	Patient status only
8	≤65 years	Reference (0)	Non-fasting	Yes	Aspirin only
9	>65 years	Patient (1)	Fasting	No	Older age + patient status + fasting
10	>65 years	Reference (0)	Fasting	Yes	Older age + fasting + aspirin
11	≤65 years	Patient (1)	Fasting	Yes	Patient status + fasting + aspirin
12	>65 years	Patient (1)	Fasting	Yes	Older age + patient status + fasting + aspirin
13	≤65 years	Patient (1)	Non-fasting	Yes	Patient status + aspirin
14	>65 years	Reference (0)	Non-fasting	Yes	Older age + aspirin
15	>65 years	Patient (1)	Non-fasting	No	Older age + patient status
16	>65 years	Patient (1)	Non-fasting	Yes	Older age + patient status + aspirin

Note. Reference (0) and Patient (1) denote PTTYPE: healthy volunteer/reference status and patient disease status (predominantly ACS/PCI), respectively. These are covariate categories, not comorbidity counts or clinical risk strata.

In standard-risk profiles, the 90 mg twice-daily regimen produced the expected model-predicted PRU trajectory under the corresponding covariate and exposure assumptions. The output was summarized as a continuous distribution rather than as the proportion within a prespecified PRU range.

Older age, the disease-status indicator, concomitant aspirin use, and fasting status altered the simulated exposure and PRU trajectories in the direction determined by the fixed PopPK and sequential PK/PD covariate relationships. These scenario differences are pharmacodynamic predictions and cannot be interpreted as evidence that a lower dose reduces clinical bleeding or preserves ischemic protection.

Across the simulated covariate profiles, the 45 mg twice-daily scenario generated a lower-intensity exposure and PRU pattern than the higher-dose scenarios under the model assumptions. Because the scenario data contain no patient-level outcomes, these results are descriptive PRU simulations only and do not support individualized dose selection.

2.6. Patient-Level UK Biobank Outcome Prediction Assessment

In the 90-day landmark analysis, the ischemic composite risk set included 713 patients with 112 events, the any diagnosis-position bleeding risk set included 725 patients with 48 events, and the all-cause death risk set included 727 patients with 129 events. The PRU-enhanced model was evaluated only as an incremental prediction model within these risk sets.

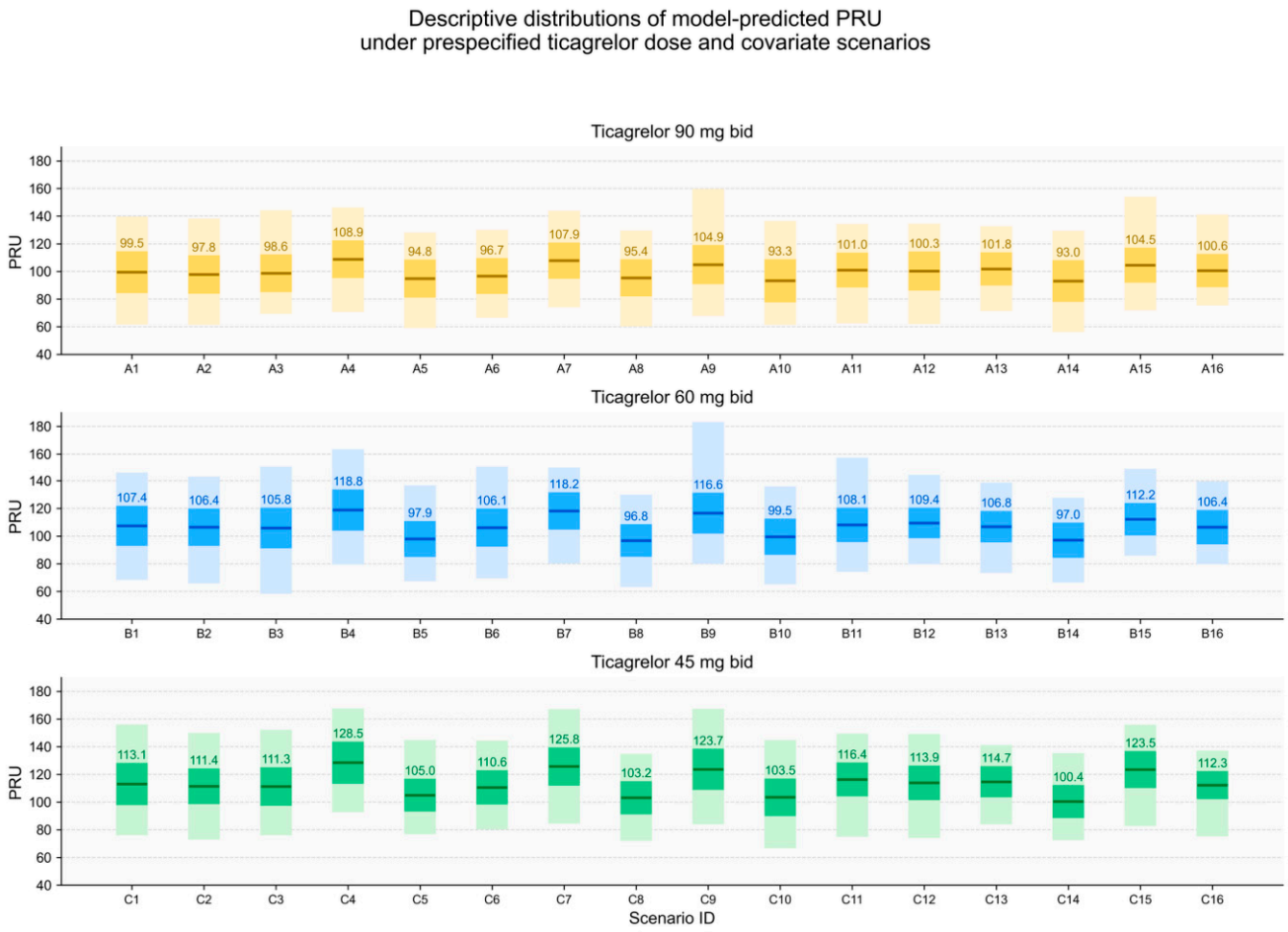


Figure 4. Distributions of model-predicted PRU under prespecified ticagrelor dosing and covariate scenarios. Light bars show the scenario-specific minimum-to-maximum range, and darker bars show the mean ± SD range; horizontal marks show the scenario mean. The simulations contain no clinical outcome risk curve, threshold, treatment interval, or dose recommendation.

Compared with M1, adding model-predicted PRU changed the apparent C-index by −0.0005 for the ischemic composite (bootstrap 95% interval, −0.0177 to 0.0099), +0.0005 for any diagnosis-position bleeding (−0.0366 to 0.0027), and +0.0018 for all-cause death (−0.0038 to 0.0036). Corresponding apparent Brier-score changes were −0.00000661, −0.00000489, and −0.00001555, and all paired-bootstrap intervals crossed zero. In the competing-risk sensitivity analysis, the bleeding C-index interval was −0.0616 to 0.0364.

The primary 90-day patient-level results are summarized in Table 3 and Figure 5. Detailed model performance, sensitivity analyses, and descriptive calibration results are provided in Supplementary Table S3. Adding model-predicted PRU did not show stable incremental predictive value for any endpoint. M1-to-M2 apparent C-index values were 0.5742 to 0.5737 for ischemic events, 0.6002 to 0.6007 for bleeding, and 0.6445 to 0.6463 for all-cause death. All paired-bootstrap intervals for C-index and Brier-score increments crossed zero. The 30-day landmark and competing-risk analyses were sensitivity analyses, and internal calibration was descriptive rather than external calibration. No threshold, treatment interval, or dose recommendation was derived.

Table 3. Primary 90-day UK Biobank patient-level outcome-prediction results.

Outcome	N/Events	M1 to M2 C-Index	Delta C-Index (95% Interval)	Delta Brier Score (95% Interval)
Ischemic composite	713/112	0.5742 to 0.5737	−0.0005 (−0.0177 to 0.0099)	−0.0000066 (−0.0000311 to 0.0000930)
Bleeding composite (any diagnosis position)	725/48	0.6002 to 0.6007	+0.0005 (−0.0366 to 0.0027)	−0.0000049 (−0.0000496 to 0.0000583)
All-cause death	727/129	0.6445 to 0.6463	+0.0018 (−0.0038 to 0.0036)	−0.0000156 (−0.0000546 to 0.0000307)

Note. M1 included age, disease-status proxy, and pre-landmark recorded supply; M2 added landmark model-predicted PRU. Intervals are paired-bootstrap 95% intervals from 500 resamples. Lower Brier scores indicate lower prediction error. PRU was model-predicted, not measured.

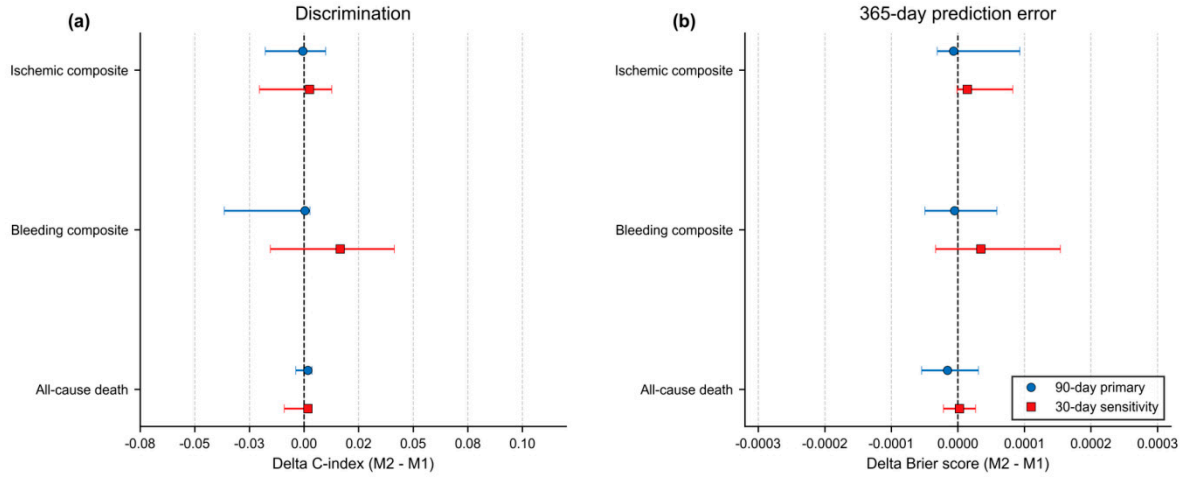


Figure 5. Incremental prediction performance in the patient-level UK Biobank analysis. (**a**) Differences in the Harrell-type C-index between M2 (M1 plus model-predicted PRU) and M1 (clinical variables plus recorded supply) for the 90-day primary and 30-day sensitivity analyses. (**b**) Corresponding differences in the 365-day Brier score. Points show apparent increments and horizontal lines show paired-bootstrap 95% intervals from 500 resamples. Zero denotes no incremental change; negative Brier-score differences favor M2. Recorded exposure was a treatment proxy, and PRU was model-predicted rather than measured.

3. Discussion

We used NONMEM to link ticagrelor dose, systemic exposure, and continuous PRU dynamics, and assessed whether model-predicted PRU improved prediction of subsequent outcomes in the UK Biobank. Patient-level PRU predictions used fixed model parameters, while treatment exposure was reconstructed from recorded prescriptions.

The UK Biobank analysis linked recorded prescription exposure and patient covariates to model-predicted PRU and subsequent outcomes. In the 90-day bleeding analysis, the PRU coefficient point estimate (HR 0.9932 per 10-unit increase) was directionally consistent with greater bleeding risk at lower PRU. The apparent C-index increased slightly and the Brier score decreased slightly after adding PRU. These small point-estimate changes did not establish stable incremental performance in the paired-bootstrap analyses.

The analysis combined 39 clinical studies and 172 group-level datasets in a population PK model of ticagrelor and AR-C124910XX. A sequential indirect-response PK/PD model used their combined molar concentration to describe the onset and offset of continuous PRU trajectories and quantify covariate effects. The locked NONMEM model was then applied to record patient-level exposure histories and evaluate for incremental prediction of subsequent outcomes. The UK Biobank analysis was internal and based on recorded prescription exposure; it was not an external validation, a measured PRU association, a causal mediation analysis, or evidence for a fixed PRU target.

Clinical outcomes after ACS and PCI are multifactorial and are influenced by coronary anatomy, plaque burden, comorbidities, procedural factors, and concomitant therapies beyond platelet reactivity [20]. Observational PRU outcome associations and randomized monitoring or de-escalation strategies have yielded context-specific findings rather than a general justification for PRU-guided dose adjustment [21–25]. PRU was retained as the pharmacodynamic summary because it is clinically interpretable and can be generated from the fixed dose–exposure–PD model. However, because PRU is derived from recorded dosing and model-supported covariates, it does not add independent measured information by construction; its value must be judged by out-of-sample prediction, calibration, and transportability.

Several covariate-effect terms and selected PD parameters, particularly EC_{50}, Kin, and Kout, had high relative uncertainty. For covariate terms, small absolute point estimates can yield large RSE values even when the absolute standard errors are modest; these values describe estimation precision rather than biological variability. For PD parameters, sparse and partly transformed platelet-function data may limit precision. These estimates therefore require cautious interpretation and do not support clinical dose decisions.

Several limitations should be noted. The UK Biobank outcome analyses had limited event counts, particularly for bleeding, and some 30-day sensitivity models had boundary estimates; the results should therefore be interpreted as internal and exploratory. No independent patient-level database with comparable dosing and time-ordered outcome fields was available for external validation. In addition, heterogeneity in endpoint definitions, follow-up, concomitant treatment, and healthcare recording may limit transportability. Tablet crushing was not consistently recorded in the source data, precluding reliable covariate assessment and limiting application to crushed-tablet administration.

High-dose records from different studies do not provide a controlled loading-versus-maintenance comparison. Dose-related changes in absorption could not be reliably separated from differences in study populations and dosing conditions. The present analysis therefore neither confirms nor excludes non-linear absorption or intestinal P-gp saturation, and its maintenance-dose simulations should not be used to infer absorption behavior after a high loading dose.

Metabolite disposition parameters were estimated with the reference Fm fixed at 0.22. Their absolute values depend on this choice. We did not perform sensitivity refits over Fm = 0.15–0.35, so the stability of parameter estimates and predictions under alternative Fm values remains untested.

Food status was represented through V and Q, which can alter the predicted concentration-time profile but do not identify a food-related change in the amount absorbed. Consequently, the model should not be interpreted as reproducing the reported food-related increase in AUC or as excluding an effect on absorption. A study designed to compare fed and fasted administration would be needed to determine the appropriate site of the food effect.

The framework provides a basis for evaluating how drug exposure and platelet inhibition contribute to clinical outcome prediction. Limited outcome events, particularly

for bleeding, and reliance on model-predicted PRU may have constrained the current assessment. Larger independent cohorts with paired measured parent-drug and metabolite concentrations, longitudinal PRU, reliable dosing and adherence records, and prospectively ascertained outcomes are needed to evaluate incremental prediction, uncertainty, calibration, and transportability before clinical application [26–28].

4. Materials and Methods

4.1. Literature Search, Study Selection, and Data Extraction

We collated published evidence on ticagrelor PK and PD. The search and extraction followed PRISMA 2020 principles [29], but the evidence set is reported as a structured literature collation rather than a formal systematic review. PubMed (https://pubmed.ncbi.nlm.nih.gov/ (accessed on 3 November 2026)) and CNKI (https://www.cnki.net/ (accessed on 3 November 2026)) were searched up to March 2024 using terms combining ticagrelor, randomized clinical trial, and acute coronary syndrome. The study-selection flow is shown in Supplementary Figure S1. Reports were selected according to study design and the availability of quantitative PK or platelet-function information. Published studies contributed aggregate PK/PD data only. An existing de-identified UK Biobank dataset available under approved access was used for the prespecified internal predictive assessment. Patient-level model inputs, recorded prescription or supply exposure, and subsequent clinical outcomes were linked within the UK Biobank. Prescription records are exposure proxies and do not establish administration, adherence, missed doses, or dose changes outside the recorded data. PRU values were generated by the fixed NONMEM model and were not measured observations.

Inclusion criteria for model-development studies were (1) adult participants (≥18 years); (2) treatment with ticagrelor, alone or as part of dual antiplatelet therapy; (3) reporting quantitative ticagrelor or AR-C124910XX concentration-time data, or compatible platelet-function data; and (4) a randomized trial or prospective/retrospective cohort with a well-defined study design. Case reports, reviews, in vitro or animal experiments, and studies without usable quantitative PK/PD data were excluded from model development.

For each included study, we extracted demographic and clinical characteristics (age range, sample size, disease status, fasting status, region, and study type), dosing regimens, parent-drug and AR-C124910XX concentration-time data, and platelet-function measurements. Directly reported PRU values were retained. When only inhibition of platelet aggregation (IPA) was reported, on-treatment PRU was calculated as follows [30]:

$$\mathrm{PRU}_{\mathrm{on-treatment}} = \left(1 - \frac{\mathrm{IPA}}{100}\right) \times \mathrm{PRU}_{\mathrm{baseline}}$$

Tablet administration modality (crushed versus intact) was not recorded in most source datasets and could not be consistently coded across the pooled records. It was therefore not evaluated as a covariate on KT or oral bioavailability. Missing modality information was not interpreted as intact-tablet administration; the model does not establish the effect of crushing on absorption.

The conversion assumes IPA is expressed as a percentage reduction from the corresponding baseline platelet-reactivity value; it was not used to equate unrelated assay platforms.

PRU_baseline was taken from the same study when reported; otherwise, the prespecified baseline value from the most closely matched population record was used and flagged as estimated. Direct PRU and converted IPA records remained distinguishable in the source-data workflow; no conversion was applied to an incompatible platelet-function platform.

Numerical data were directly extracted; graphically presented data were digitized using WebPlotDigitizer software (version 4.6) by one researcher for consistency. Key characteristics of the 39 collated studies, extracted quantitative data, and risk-of-bias assessments are summarized in Supplementary Table S1; model-input examples are provided in Supplementary Table S2.

4.2. Population Pharmacokinetic Model Development

Noncompartmental analysis (NCA) was first conducted on concentration-time data from key studies to define empirical PK parameter ranges and guide structural model selection. The final population PK and sequential PK/PD models were implemented in NONMEM (version 7.4.4). First-order, lag-time, and transit absorption structures were compared with alternative distribution-elimination structures. In the selected model, the oral dose enters a dosing compartment (Aa/DEPOT) and passes sequentially through three transit compartments (T1, T2, and T3) before entering the parent-drug central compartment. All four transfers share the first-order transit rate constant KT; no separate ka or explicit lag-time parameter is used. Ticagrelor and its active metabolite each have central and peripheral distribution compartments. Model development and patient-level prediction were treated as separate analyses [31]. The patient-level control stream applied the locked parameter state and did not repeat parameter estimation or structural model comparison [32,33].

Dose-dependent absorption and intestinal P-glycoprotein (P-gp) saturation were not formally tested. Although the literature collation contains high-dose and some loading-dose records, the model-development input does not separately identify loading and maintenance administrations. The linear transit structure was retained to describe the absorption time course in the pooled data; it does not represent a saturable transporter mechanism.

Variability in the model-development records was represented with exponential random effects and was not interpreted as patient-specific interindividual variability. Residual error for the concentration records was modeled on a log-additive scale. Concentrations of ticagrelor and AR-C124910XX were converted to total molar concentration and analyzed on a common scale to reflect their combined pharmacologic effect [6,34].

Candidate covariates were prespecified from pharmacologic plausibility and prior evidence. They included age, body weight, body mass index (BMI), sex, fasting status, concomitant aspirin use, and disease status. Covariates were modeled as categorical or continuous variables as appropriate; continuous covariates were median-normalized. Forward inclusion used alpha = 0.05, and backward elimination used alpha = 0.01, with effect magnitude, clinical relevance, and pharmacologic plausibility also considered. The selected relationships were included in the final NONMEM control stream for patient-level prediction. Covariate selection was not repeated at the patient level.

The final covariate structure used indicators for age group (AGEE), disease/patient status (PTTYPE), fasting status (FAFE), and concomitant aspirin (ASP). Age group affected parent-drug clearance (CL) and the metabolite formation fraction (Fm); disease status affected CL, peripheral volume (Vp), and EC_{50}; and aspirin affected CL. Fasting status was included (FAFE = 0, fasting; FAFE = 1, non-fasting), with retained effects on central volume (V) and intercompartmental clearance (Q). The implemented relationships were $V = TVV \times \exp(0.371734 \times FAFE) \times \exp(ETA_V)$ and $Q = TVQ \times \exp(-0.820691 \times FAFE) \times \exp(ETA_Q)$. The absorption chain uses KT, without a separate ka; neither KT nor oral bioavailability has a food-status term. Body weight, BMI, and sex do not appear in the final control streams. The V and Q terms represent empirical associations in the pooled oral concentration-time data and are not interpreted as evidence that food changes physiological distribution. The pooled data do not adequately distinguish a food effect on absorption from differences between studies and clinical populations. The retained

parameterization therefore does not establish that food effects on KT or bioavailability were tested and excluded.

The reference-group typical metabolite formation fraction (Fm) was fixed at 0.22, following the value used by Amilon et al. in their ticagrelor parent-metabolite population PK/PD model [35]. They set the fraction of ticagrelor metabolized to AR-C124910XX to 0.22 and cited AstraZeneca data on file as its source. In our model, 0.22 is the fixed reference-group typical value; the age-group term and random effect on Fm were retained.

Fixing the reference Fm defines the scale for estimating metabolite disposition parameters in the sequential model; the available pooled data do not independently establish its absolute value. This assumption does not establish uniform CYP3A activity across disease states or co-medications.

4.3. Sequential PK/PD Modeling of PRU Dynamics

Following PopPK model finalization, sequential PK/PD analysis was performed using model-predicted exposure trajectories. PopPK parameters were held at the finalized values, and the PD model used the combined molar concentration of ticagrelor and AR-C124910XX as its exposure driver. The PD endpoint was standardized PRU, with longitudinal PRU profiles representing dynamic platelet inhibition.

An indirect-response model was adopted to capture the gradual onset and offset of ticagrelor's antiplatelet effect, wherein total molar concentration increases the PRU loss term. The no-drug baseline PRU is defined by Kin/Kout; the model parameters therefore comprised E_{max}, EC_{50}, Kin, and Kout rather than an independently estimated baseline PRU parameter.

4.4. Model Evaluation and Qualification

All patient-level PRU predictions were generated with the final fixed-parameter NONMEM implementation. The patient-level control stream used the locked model structure, parameter values, and covariate relationships; it did not re-estimate parameters, compare structures, or select covariates. GOF, VPC, and bootstrap outputs describe the model-development analysis and were not generated by a separate patient-level estimation step. Prediction-corrected visual predictive checks were used as model-development diagnostics [36].

4.5. Patient-Level Clinical Outcome Prediction Assessment

We used the existing de-identified UK Biobank data under a prespecified analysis protocol to test whether model-predicted PRU contributes to patient-level clinical outcome prediction. The analysis examined the incremental information from a continuous PRU summary after accounting for core clinical variables and recorded medication exposure.

The UK Biobank analysis included 731 participants with complete model-supported inputs. In the source model-development data, PTTYPE was the binary disease/patient-status indicator (0, healthy volunteer/reference status; 1, patient disease status, predominantly ACS/PCI), not a generic count or indicator of comorbidities. For UK Biobank implementation, PTTYPE = 1 was assigned when an ACS diagnosis or PCI procedure was recorded within 30 days before the first valid ticagrelor prescription; absence of such recent coded evidence was assigned 0 and interpreted as a rule-based proxy rather than directly observed stable disease. Ticagrelor 60 or 90 mg prescriptions with a valid issue date and positive tablet quantity were mapped to twice-daily use because frequency was not recorded. Supply duration was quantity divided by two, and intervals were left-closed and right-open. Same-strength overlaps were merged by interval union rather than stockpiled; discordant-strength overlaps were flagged and excluded from the strict exposure input. FAFE was mapped from

recorded fasting duration: FAFE = 0 for fasting duration ≥ 8 h and FAFE = 1 for fasting duration < 8 h; missing fasting duration was not imputed in the primary mapping and was retained for sensitivity handling. Concomitant aspirin was derived from overlapping 75 or 150 mg recorded supply windows. These variables represent recorded exposure proxies, not administration or adherence.

A 90-day landmark after the first valid recorded ticagrelor prescription was prespecified as the primary analysis time point. Eligible participants were alive, under observation, and free of the endpoint at the landmark; continued recorded supply coverage at day 90 was not required. Only prescriptions issued on or before the landmark entered NONMEM. The primary PRU summary was model-predicted PRU at the landmark; the day 1–90 time-weighted average was a sensitivity summary. A 30-day landmark was a time-point sensitivity analysis.

Endpoints were modeled separately. The ischemic composite comprised first post-landmark acute myocardial infarction (primary-position ICD-10 I21–I22), ischemic stroke (primary-position I63), or cardiovascular death with a primary cause in I00–I99. The any diagnosis-position bleeding composite comprised first intracranial hemorrhage (I60–I62) or gastrointestinal hemorrhage (K92.0–K92.2) in any HES diagnosis position; a primary-position definition was retained as a specificity analysis. All-cause death used the death registry. HES event dates used epistart, or admidate when epistart was unavailable, and were interpreted as episode-date proxies rather than exact onset dates. Same-day landmark events were excluded from post-landmark outcomes.

Three nested Cox models were fitted: M0 included age and PTTYPE; M1 added pre-landmark recorded supply days divided by 90; and M2 added landmark model-predicted PRU divided by 10. For non-fatal endpoints, death was treated as a competing event in cause-specific sensitivity analyses. Follow-up ended at the first qualifying event, recorded loss/withdrawal, death for non-fatal endpoints, or the official HES administrative cutoff for the participant's data source (England, 31 March 2023; Scotland, 31 August 2022; Wales, 31 May 2022). Performance measures were the Harrell-type C-index over available post-landmark follow-up, a descriptive complete-status Brier score at 365 days, and 10-group descriptive calibration, selected to characterize discrimination, prediction error, and calibration rather than to claim external validation [37–39]. For the Brier score and calibration, participants were evaluable only if the endpoint occurred by day 365 or event-free follow-up reached at least day 365; no inverse-probability-of-censoring weighting was applied. Internal uncertainty was assessed with 500 participant-level bootstrap samples drawn with replacement from each endpoint-specific risk set. M1 and M2 were refitted in every paired resample and evaluated on the original risk set using the baseline hazard estimated in that resample. M2-minus-M1 C-index and Brier increments used identical resamples, with 95% intervals defined by the 2.5th and 97.5th percentiles. Random seeds were 20260829 for the ordinary Cox analysis and 202608314 for the competing-risk sensitivity analysis. No fixed PRU threshold or interval was used.

The stability of PRU representation was examined by comparing landmark PRU with the time-weighted PRU sensitivity summary. Model complexity was restricted by the observed event counts. The 90-day analysis was the primary analysis; the 30-day analysis was reported only as a time-point sensitivity analysis because some PRU-containing models showed boundary estimates and unstable information.

The patient-level outcome analysis was separate from the aggregate data simulations. The simulations described continuous PRU trajectories under prespecified dose and covariate scenarios; they were not used to estimate clinical event risk or dose benefit.

4.6. Model-Based PRU Simulation Scenarios

The final population PK and sequential PK/PD models were implemented in NONMEM. Model-development simulations described continuous PRU trajectories under prespecified ticagrelor dosing scenarios. They did not estimate observed clinical event probabilities.

Simulation scenarios included ticagrelor maintenance regimens of 90 and 60 mg twice daily and an exploratory 45 mg twice-daily regimen. Published dose-comparison and de-escalation studies provide the context for these regimens but do not validate the simulated 45 mg scenario [40,41]. Prespecified clinical profiles combined age, disease status, fasting status, and concomitant aspirin use (Table 2). The scenarios described model-predicted PRU distributions and were not used to recommend a dose.

Each scenario included 2500 virtual individuals and used the final model parameter and variance state. The patient-level NONMEM run used fixed typical parameters, observed prescription records, and no simulated population variability.

Primary outputs were continuous PRU time trajectories and scenario-specific means, standard deviations, minima, and maxima. No fixed PRU interval, threshold, or interval-coverage metric was used.

Scenario results were summarized by the mean, standard deviation, minimum, and maximum of the continuous PRU values. Dose comparisons were descriptive and were not used to estimate clinical event risk, clinical benefit, or dose adjustment.

Table 2 lists the prespecified covariate combinations used in the simulation scenarios and does not provide clinical dose recommendations. Maintenance regimens of 90, 60, and 45 mg twice daily were compared using continuous model-predicted PRU values. These outputs were separate from the current fixed-parameter patient-level NONMEM run (Figure 4).

4.7. Use of Generative Artificial Intelligence

OpenAI Codex (GPT-5, accessed August 2026) was used to assist with language editing, code auditing, document consistency checks, and preparation of reproducibility documentation. It was not used to generate or alter patient-level data or to determine statistical results. The authors reviewed and verified all outputs and take full responsibility for the content of the study.

5. Conclusions

We established a NONMEM-based framework linking ticagrelor dosing, parent-drug and metabolite exposure, and PRU dynamics to patient-level outcome prediction assessment. Although an incremental predictive benefit was not established in the current cohort, the framework provides a basis for prospective evaluation. Larger independent studies with paired measured PK and PD, reliable dosing records, and sufficient clinical outcome events are needed to validate its potential to inform individualized ticagrelor dosing.

Supplementary Materials: The following supporting information can be downloaded at: https://www.mdpi.com/article/10.3390/ph19111780/s1, Supplementary Methods; Supplementary Table S1: Literature collation and risk-of-bias summary; Supplementary Table S2: Model-input examples; Supplementary Table S3: Aggregate patient-level outcome-prediction results; Supplementary Figure S1: Study-selection flow; and NONMEM Codes S1–S3, covering parent PK, metabolite PK, and sequential PRU PD. Controlled UK Biobank participant-level data and patient-level statistical analysis scripts are not included.

Author Contributions: Conceptualization, D.L. and C.C.; methodology, S.D., J.C., D.L. and C.C.; software, S.D.; validation, S.D. and J.C.; formal analysis, S.D.; investigation, S.D. and J.C.; data curation, S.D.; writing—original draft preparation, S.D.; writing—review and editing, J.C., D.L. and

C.C.; visualization, S.D.; supervision, J.C., D.L. and C.C.; project administration, D.L. and C.C. All authors have read and agreed to the published version of the manuscript.

Funding: This research was funded by the Beijing Research Ward Excellence Program, grant number BRWEP2024W014090208.

Institutional Review Board Statement: The UK Biobank study was conducted in accordance with the Declaration of Helsinki and approved by the North West-Haydock Research Ethics Committee (REC reference 21/NW/0157; approval date 18 June 2021). The present secondary analysis was conducted under UK Biobank application 258644. No new participants were recruited.

Informed Consent Statement: Informed consent was obtained from all subjects involved in the UK Biobank study. No additional participant consent was required for this secondary analysis of de-identified data.

Data Availability Statement: The data presented in this study are available on request from the corresponding author due to privacy and participant confidentiality. The UK Biobank data used in this study are subject to application and approval, and are not publicly available.

Acknowledgments: During the preparation of this manuscript and study, the authors used OpenAI Codex (GPT-5, accessed August 2026) for language editing, code auditing, document consistency checks, and preparation of reproducibility documentation. The authors reviewed and edited the outputs and take full responsibility for the content of this publication.

Conflicts of Interest: The authors declare no conflicts of interest.

References

1. Bonaca, M.P.; Bhatt, D.L.; Cohen, M. Long-term use of ticagrelor in patients with prior myocardial infarction (PEGASUS-TIMI 54). *N. Engl. J. Med.* **2015**, *372*, 1791–1800. [CrossRef] [PubMed]
2. Virani, S.S.; Newby, L.K.; Arnold, S.V. 2023 AHA/ACC/ACCP/ASPC/NLA/PCNA Guideline for the Management of Patients With Chronic Coronary Disease. *Circulation* **2023**, *148*, e9–e119. [CrossRef] [PubMed]
3. Alagna, G.; Mazzone, P.; Contarini, M. Dual antiplatelet therapy with parenteral P2Y12 inhibitors: Rationale, evidence, and future directions. *J. Cardiovasc. Dev. Dis.* **2023**, *10*, 163. [CrossRef] [PubMed]
4. Valgimigli, M. 'Ten Commandments' of the 2017 ESC DAPT focused update Guidelines. *Eur. Heart J.* **2018**, *39*, 186. [CrossRef] [PubMed]
5. Wallentin, L.; Becker, R.C.; Budaj, A. Ticagrelor versus clopidogrel in patients with acute coronary syndromes (PLATO). *N. Engl. J. Med.* **2009**, *361*, 1045–1057. [CrossRef] [PubMed]
6. Husted, S.; Emanuelsson, H.; Heptinstall, S. Pharmacodynamics, pharmacokinetics, and safety of the oral reversible P2Y12 antagonist AZD6140 with aspirin in patients with atherosclerosis: A double-blind comparison to clopidogrel with aspirin. *Eur. Heart J.* **2006**, *27*, 1038–1047. [CrossRef] [PubMed]
7. Teng, R. Ticagrelor: Pharmacokinetic, Pharmacodynamic and Pharmacogenetic Profile: An Update. *Clin. Pharmacokinet.* **2015**, *54*, 1125–1138. [CrossRef] [PubMed]
8. Esteve-Pastor, M.A.; Ruíz-Nodar, J.M.; Orenes-Piñero, E.; Rivera-Caravaca, J.M.; Quintana-Giner, M.; Véliz-Martínez, A.; Tello-Montoliu, A.; PerniasEscrig, V.; Rollán, M.S.; Vicente-Ibarra, N.; et al. Temporal Trends in the Use of Antiplatelet Therapy in Patients With Acute Coronary Syndromes. *J. Cardiovasc. Pharmacol. Ther.* **2018**, *23*, 57–65. [CrossRef] [PubMed]
9. Jacobsen, M.R.; Jabbari, R.; Engstrøm, T.; Grove, E.L.; Glinge, C.; Pedersen, F.; Holmvang, L.; Køber, L.; Torp-Pedersen, C.; Maeng, M.; et al. Bleeding risk and P2Y12 inhibitors in all-comer patients with ST-segment elevation myocardial infarction treated with percutaneous coronary intervention: A single-centre cohort study. *Eur. Heart J. Cardiovasc. Pharmacother.* **2023**, *9*, 617–626. [CrossRef] [PubMed]
10. Tam, C.C.; Tse, H.F. Antiplatelet therapy aims and strategies in Asian patients with acute coronary syndrome or stable coronary artery disease. *J. Clin. Med.* **2022**, *11*, 7440. [CrossRef] [PubMed]
11. Marxer, C.A.; Hjemdahl, P.; Carrero, J.J.; Fu, E.L. Comparative effectiveness and safety of dual antiplatelet therapy with ticagrelor vs. clopidogrel in older adults with acute coronary syndrome: A target trial emulation study. *Eur. Heart J. Cardiovasc. Pharmacother.* **2025**, *11*, 500–508. [CrossRef] [PubMed]
12. Bonello, L.; Tantry, U.S.; Marcucci, R.; Blindt, R.; Angiolillo, D.J.; Becker, R.; Bhatt, D.L.; Cattaneo, M.; Collet, J.P.; Cuisset, T.; et al. Consensus and future directions on the definition of high on-treatment platelet reactivity to adenosine diphosphate. *J. Am. Coll. Cardiol.* **2010**, *56*, 919–933. [CrossRef] [PubMed]

13. Wang, H.; Qi, J.; Li, Y. Pharmacodynamics and pharmacokinetics of ticagrelor vs. clopidogrel in patients with acute coronary syndromes and chronic kidney disease. *Br. J. Clin. Pharmacol.* **2018**, *84*, 88–96. [CrossRef] [PubMed]
14. Zlatanovic, P.; Wong, K.H.F.; Kakkos, S.K.; Twine, C.P. A Systematic Review and Meta-Analysis on the Impact of High On-Treatment Platelet Reactivity on Clinical Outcomes for Patients Taking ADP Receptor Inhibitors Following Lower Limb Arterial Endovascular Intervention. *Eur. J. Vasc. Endovasc. Surg.* **2022**, *63*, 91–101. [CrossRef] [PubMed]
15. Hochholzer, W.; Trenk, D.; Frundi, D.; Neumann, F.J. Whole blood aggregometry for evaluation of the antiplatelet effects of clopidogrel. *Thromb. Res.* **2007**, *119*, 285–291. [CrossRef] [PubMed]
16. Collet, J.P.; Cuisset, T.; Rangé, G.; Cayla, G.; Elhadad, S.; Pouillot, C.; Henry, P.; Motreff, P.; Carrié, D.; Boueri, Z.; et al. Bedside monitoring to adjust antiplatelet therapy for coronary stenting. *N. Engl. J. Med.* **2012**, *367*, 2100–2109. [CrossRef] [PubMed]
17. Karaźniewicz-Łada, M.; Danielak, D.; Burchardt, P.; Kruszyna, L.; Komosa, A.; Lesiak, M.; Główka, F. Clinical pharmacokinetics of clopidogrel and its metabolites in patients with cardiovascular diseases. *Clin. Pharmacokinet.* **2014**, *53*, 155–164. [CrossRef] [PubMed]
18. Liu, S.; Xue, L.; Shi, X.; Sun, Z.; Zhu, Z.; Zhang, X.; Tian, X. Population pharmacokinetics and pharmacodynamics of ticagrelor and AR-C124910XX in Chinese healthy male subjects. *Eur. J. Clin. Pharmacol.* **2018**, *74*, 745–754. [CrossRef] [PubMed]
19. Li, H.; Guo, J.; Carlson, G.F.; Teng, R. Pharmacodynamics, pharmacokinetics, and safety of ticagrelor in Chinese patients with stable coronary artery disease. *Br. J. Clin. Pharmacol.* **2016**, *82*, 352–361. [CrossRef] [PubMed]
20. Byrne, R.A.; Rossello, X.; Coughlan, J.J.; Barbato, E.; Berry, C.; Chieffo, A.; Claeys, M.J.; Dan, G.-A.; Dweck, M.R.; Galbraith, M.; et al. 2023 ESC Guidelines for the management of acute coronary syndromes. *Eur. Heart J. Acute Cardiovasc. Care* **2024**, *13*, 55–161. [CrossRef] [PubMed]
21. Price, M.J.; Angiolillo, D.J.; Teirstein, P.S.; Lillie, E.; Manoukian, S.V.; Berger, P.B.; Tanguay, J.-F.; Cannon, C.P.; Topol, E.J. Platelet reactivity and cardiovascular outcomes after percutaneous coronary intervention: A time-dependent analysis of the GRAVITAS trial. *Circulation* **2011**, *124*, 1132–1137. [CrossRef] [PubMed]
22. Price, M.J.; Berger, P.B.; Teirstein, P.S.; Tanguay, J.F.; Angiolillo, D.J.; Spriggs, D.; Puri, S.; Robbins, M.; Garratt, K.N.; Bertrand, O.F.; et al. Standard- vs high-dose clopidogrel based on platelet function testing after percutaneous coronary intervention: The GRAVITAS randomized trial. *JAMA* **2011**, *305*, 1097–1105. [CrossRef] [PubMed]
23. Cayla, G.; Cuisset, T.; Silvain, J.; Leclercq, F.; Manzo-Silberman, S.; Saint-Etienne, C.; Delarche, N.; Bellemain-Appaix, A.; Range, G.; El Mahmoud, R.; et al. Platelet function monitoring to adjust antiplatelet therapy in elderly patients stented for an acute coronary syndrome (ANTARCTIC): An open-label, blinded-endpoint, randomised controlled trial. *Lancet* **2016**, *388*, 2015–2022. [CrossRef] [PubMed]
24. Sibbing, D.; Aradi, D.; Jacobshagen, C.; Gross, L.; Trenk, D.; Geisler, T.; Orban, M.; Hadamitzky, M.; Merkely, B.; Kiss, R.G.; et al. Guided de-escalation of antiplatelet treatment in patients with acute coronary syndrome undergoing percutaneous coronary intervention (TROPICAL-ACS): A randomised, open-label, multicentre trial. *Lancet* **2017**, *390*, 1747–1757. [CrossRef] [PubMed]
25. Aradi, D.; Gross, L.; Trenk, D.; Geisler, T.; Merkely, B.; Kiss, R.G.; Komócsi, A.; Dézsi, C.A.; Ruzsa, Z.; Ungi, I.; et al. Platelet reactivity and clinical outcomes in acute coronary syndrome patients treated with prasugrel and clopidogrel: A pre-specified exploratory analysis from the TROPICAL-ACS trial. *Eur. Heart J.* **2019**, *40*, 1942–1951. [CrossRef] [PubMed]
26. Royston, P.; Altman, D.G. External validation of a Cox prognostic model: Principles and methods. *BMC Med. Res. Methodol.* **2013**, *13*, 33. [CrossRef] [PubMed]
27. Collins, G.S.; Reitsma, J.B.; Altman, D.G.; Moons, K.G. Transparent reporting of a multivariable prediction model for individual prognosis or diagnosis (TRIPOD): The TRIPOD statement. *Circulation* **2015**, *131*, 211–219. [CrossRef] [PubMed]
28. Kluwe, F.; Michelet, R.; Huisinga, W.; Zeitlinger, M.; Mikus, G.; Kloft, C. Towards model-informed precision dosing of voriconazole: Challenging published voriconazole nonlinear mixed-effects models with real-world clinical data. *Clin. Pharmacokinet.* **2023**, *62*, 1461–1477. [CrossRef] [PubMed]
29. Page, M.J.; McKenzie, J.E.; Bossuyt, P.M. The PRISMA 2020 statement: An updated guideline for reporting systematic reviews. *BMJ* **2021**, *372*, n71. [CrossRef] [PubMed]
30. Lordkipanidzé, M.; Pharand, C.; Nguyen, T.A.; Schampaert, E.; Diodati, J.G. Assessment of VerifyNow P2Y12 assay accuracy in evaluating clopidogrel-induced platelet inhibition. *J. Thromb. Thrombolysis* **2008**, *26*, 170–176.
31. Wang, Y.; Zhu, H.; Madabushi, R.; Liu, Q.; Huang, S.M.; Zineh, I. Model-informed drug development: Current US regulatory practice and future considerations. *Clin. Pharmacol. Ther.* **2019**, *105*, 899–911. [CrossRef] [PubMed]
32. Liu, Y.; Kuang, Y.; Hai, M. Model-Informed Dosing Regimen of Ticagrelor in Chinese Patients With Acute Coronary Syndrome. *Clin. Pharmacol. Ther.* **2023**, *114*, 1342–1349. [CrossRef] [PubMed]
33. Shin, Y.; Chae, D.; Park, K. Development of a population pharmacokinetic model and optimal dosing regimen of leflunomide in Korean population. *Eur. J. Pharm. Sci.* **2023**, *184*, 106402. [CrossRef] [PubMed]
34. Teng, R.; Oliver, S.; Hayes, M.A.; Butler, K. Absorption, distribution, metabolism, and excretion of ticagrelor in healthy subjects. *Drug Metab. Dispos.* **2010**, *38*, 1514–1521. [CrossRef] [PubMed]

35. Amilon, C.; Niazi, M.; Berggren, A.; Åstrand, M.; Hamrén, B. Population Pharmacokinetics/Pharmacodynamics of Ticagrelor in Children with Sickle Cell Disease. *Clin. Pharmacokinet.* **2019**, *58*, 1295–1307. [CrossRef] [PubMed]
36. Bergstrand, M.; Hooker, A.C.; Wallin, J.E.; Karlsson, M.O. Prediction-corrected visual predictive checks for diagnosing nonlinear mixed-effects models. *AAPS J.* **2011**, *13*, 143–151. [CrossRef] [PubMed]
37. Steyerberg, E.W.; Vickers, A.J.; Cook, N.R.; Gerds, T.; Gonen, M.; Obuchowski, N.; Pencina, M.J.; Kattan, M.W. Assessing the performance of prediction models: A framework for traditional and novel measures. *Epidemiology* **2010**, *21*, 128–138. [CrossRef] [PubMed]
38. Uno, H.; Cai, T.; Pencina, M.J.; D'Agostino, R.B.; Wei, L.J. On the C-statistics for evaluating overall adequacy of risk prediction procedures with censored survival data. *Stat. Med.* **2011**, *30*, 1105–1117. [CrossRef] [PubMed]
39. Graf, E.; Schmoor, C.; Sauerbrei, W.; Schumacher, M. Assessment and comparison of prognostic classification schemes for survival data. *Stat. Med.* **1999**, *18*, 2529–2545. [CrossRef]
40. Piccolo, R.; Simonetti, F.; Avvedimento, M.; Cutillo, M.; Canonico, M.E.; Conti, V.; Gargiulo, G.; Paolillo, R.; Piaz, F.D.; Filippelli, A.; et al. Ticagrelor 60 vs. 90 mg in elderly ACS patients undergoing PCI: A randomized, crossover trial. *Eur. Heart J. Cardiovasc. Pharmacother.* **2024**, *10*, 578–587. [CrossRef] [PubMed]
41. Tavenier, A.H.; Mehran, R.; Chiarito, M.; Cao, D.; Pivato, C.A.; Nicolas, J.; Beerkens, F.; Nardin, M.; Sartori, S.; Baber, U.; et al. Guided and unguided de-escalation from potent P2Y12 inhibitors among patients with acute coronary syndrome: A meta-analysis. *Eur. Heart J. Cardiovasc. Pharmacother.* **2022**, *8*, 492–502. [CrossRef] [PubMed]

Disclaimer/Publisher's Note: The statements, opinions and data contained in all publications are solely those of the individual author(s) and contributor(s) and not of MDPI and/or the editor(s). MDPI and/or the editor(s) disclaim responsibility for any injury to people or property resulting from any ideas, methods, instructions or products referred to in the content.